ORIGINAL ARTICLE

Amyloid-β mediates intestinal dysfunction and enteric neurons loss in Alzheimer's disease transgenic mouse

Guoqiang Liu[1] · Quntao Yu[2,3] · Houze Zhu[2,3] · Bo Tan[2,3] · Hongyan Yu[2,3] · Xinyan Li[2,3] · Youming Lu[2,3,4] · Hao Li[3,4]

Abstract

Alzheimer's disease (AD) is traditionally considered as a brain disorder featured by amyloid-β (Aβ) deposition. The current study on whether pathological changes of AD extend to the enteric nervous system (ENS) is still in its infancy. In this study, we found enteric Aβ deposition, intestinal dysfunction, and colonic inflammation in the young APP/PS1 mice. Moreover, these mice exhibited cholinergic and nitrergic signaling pathways damages and enteric neuronal loss. Our data show that Aβ42 treatment remarkably affected the gene expression of cultured myenteric neurons and the spontaneous contraction of intestinal smooth muscles. The intra-colon administration of Aβ42 induced ENS dysfunction, brain gliosis, and β-amyloidosis-like changes in the wild-type mice. Our results suggest that ENS mirrors the neuropathology observed in AD brains, and intestinal pathological changes may represent the prodromal events, which contribute to brain pathology in AD. In summary, our findings provide new opportunities for AD early diagnosis and prevention.

Keywords Alzheimer's disease · Amyloid-β · Gastrointestinal motility · Enteric neuronal loss · Intestinal contraction

Introduction

Alzheimer's disease (AD) is characterized by a progressive loss of memory and cognitive function as well as the amyloid-β (Aβ) deposition and neuronal loss. Currently, early diagnosis and effective treatment are still great challenges for AD [1]. For a long time, the research on AD has focused on the lesions of the central nervous system (CNS).

Guoqiang Liu and Quntao Yu are co-first authors.

✉ Youming Lu
  lym@hust.edu.cn

✉ Hao Li
  lihhhhao@hust.edu.cn

[1] Medical College, Hubei University for Nationalities, Enshi 445000, Hubei, China

[2] Department of Physiology, School of Basic Medicine and Tongji Medical College, Huazhong University of Science and Technology, Wuhan 4030030, China

[3] Wuhan Center of Brain Science, Huazhong University of Science and Technology, Wuhan 430030, China

[4] Department of Pathophysiology, School of Basic Medicine and Tongji Medical College, Huazhong University of Science and Technology, Wuhan 430030, China
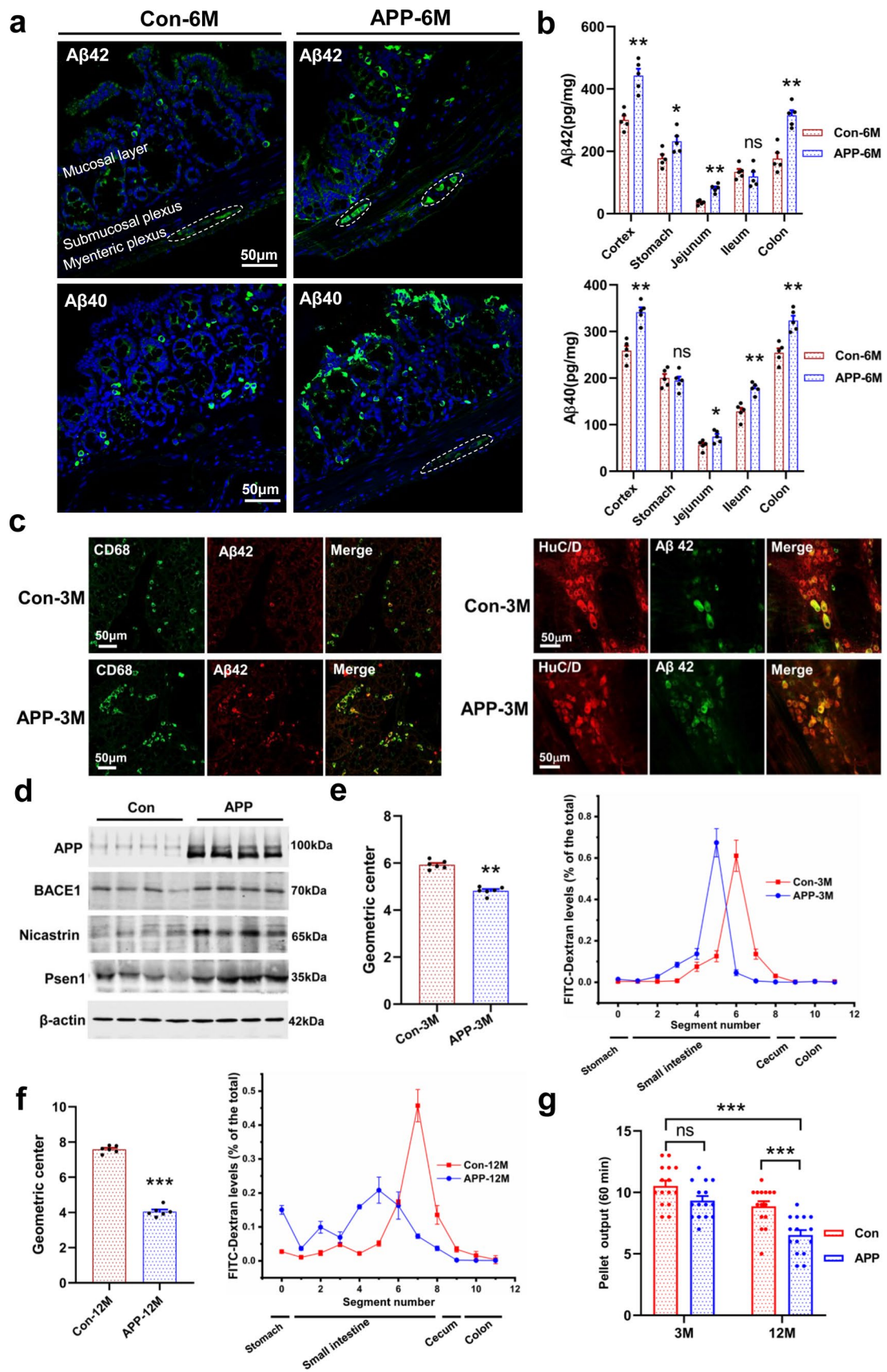
However, a series of peripheral abnormalities such as systemic inflammation, metabolic dysfunction, and microbiota disturbance have been reported in AD patients [2]. Peripheral organs such as kidney, liver, muscle, and gut produce Aβ [3], and blood cell-produced Aβ has been reported to induce behavioral deficits and AD-type pathologies [4]. These findings suggest that interactions between the periphery and brain play an important role in AD pathology.

Emerging studies suggest that gastrointestinal (GI) dysfunction, gut dysbiosis, and enteric neuropathy are associated with risk of developing AD, autism spectrum disorders, and Parkinson's disease (PD) [5, 6]. For AD, dextran sulfate sodium-induced gut inflammation exacerbates Aβ plaque load in the hippocampus and temporal cortex [7] and gut dysbiosis accelerates AD pathology in the young 3xTg mice [8] and *Drosophila* AD model [9]. In addition, a study reported that the transfer of healthy microbiota decreased the amyloid and Tau pathology in ADLPAPT transgenic mouse [10]. Accumulating evidence from animal models and epidemiological studies suggest that GI symptoms might not be secondary to the CNS degeneration; instead, GI tract and enteric nervous system (ENS) might act as a potential targets of neurological disorders [11].

The ENS, which plays an essential role in local control and fine coordination of GI function, has a high homology

◄**Fig. 1** Enteric Aβ deposition and GI motility impairment in the APP/PS1 mice. **a** Representative micrographs showed the Aβ40 (Biolegend: 805409) and Aβ42 (Biolegend: 805501) deposition in the colonic mucosal layer and myenteric plexus of 6-month-old APP/PS1 mice and littermate controls, $N=5$/group. The results of quantitative analysis were shown in the Fig. S2a. **b** Quantitative analysis of the Aβ42 and Aβ40 levels in the GI tract of 6-month-old APP/PS1 mice and littermate controls by ELISA. $N=5$/group. Data are presented as mean±SEM, *$P<0.05$, **$P<0.01$. The "ns" represents no significance. **c** Immunofluorescence characterization of the Aβ42-positive cells in the colonic mucosal layer and myenteric plexus in 3-month-old APP/PS1 mice and littermate controls, $N=5$/group. The Anti-Aβ42 antibody (Abcam: ab10148) was used. **d** Expression of proteins involved in Aβ generation measured by Western blotting in the colon of 12-month-old APP/PS1 mice and littermate controls, $N=8$/group. Amyloid precursor protein: APP; beta-secretase: BACE1; gamma-secretase: Presenilin1 (Psen1) and Nicastrin. **e**, **f** GI transit assay in vivo in 3-month-old (**e**) and 12-month-old (**f**) APP/PS1 mice and littermate controls, $N=6$/group. The geometric center of FITC-dextran and the distribution of fluorescent marker along the GI tract were shown in the figure. Data are presented as mean±SEM, unpaired t test, **$P<0.01$. **g** Stool characteristics were changed in the 3- and 12-month-old APP/PS1 mice as compared with the littermate controls, $N=15$/group. Data are presented as mean±SEM. Statistical significance was determined using two-way ANOVA, $F_{(1, 28)}=25.91$, *$P<0.05$, ***$P<0.001$

with CNS in transcriptional programs, morphology and neurochemistry [12]. Therefore, it is not surprising that ENS may be also damaged by a pathogenic mechanism leading to CNS disorders. In PD mouse model, α-synuclein aggregation has been found in the enteric neurons and is associated with colonic dysmotility [13], and these pathologic changes precede degeneration of nigrostriatal dopaminergic neurons [14, 15]. Aβ was considered as a critical initiator of AD that results in cognitive impairment and neuronal death via accumulation and aggregation [16]. Recent research suggests that amyloid precursor protein (βAPP) and its metabolite, Aβ, are normally expressed in the intestine of AD transgenic mice [17, 18]; APP was found to be involved in modulating immunity and cholesterol uptake [19, 20]. An early report shows the immunoreactivity of βAPP in the GI tract of AD patients [21]. These findings raise exciting new questions: Is there any intestinal dysfunction and ENS damage in AD mice? If yes, what is the role of intestinal Aβ in these changes? What is the relationship between intestinal pathological changes and brain Aβ deposition? Currently, studies about these issues are still limited. Understanding the characteristic pathological changes initially occur in GI tract will provide new insight into early diagnosis and treatment of AD.

In this study, we observed enteric intraneuronal Aβ deposition and GI transit impairment in the young APP/PS1 mice, and found that cholinergic and nitrergic neurons were lost with aging. Our data revealed that Aβ deposition and bacterial LPS contribute to enteric neurons apoptosis and neuroinflammation. Furthermore, we found that Aβ treatment has a significant influence on the spontaneous contraction of intestinal smooth muscle in vitro and demonstrated that intra-colon administration of Aβ42 resulted in ENS dysfunction and cerebral β-amyloidosis in the wild-type (WT) mice. Taken together, our results suggested that the ENS reproduced the typical pathological features described in the CNS, and proposed that the intestinal symptoms and ENS alterations are likely to be the earliest pathological potential events in AD, which contribute to the development of brain pathology.

Results

Aβ deposition in the intestinal mucosal layer and ENS

Aβ deposition was thought as the prominent pathological hallmark in AD brains. The APP/PS1 transgenic mice exhibited Aβ deposition in the hippocampus and cortex at 6 months of age, and the plaque load increased with age (Fig. S1). In this study, we found an increased intracellular Aβ40 and Aβ42 deposition in the colonic myenteric plexuses and mucosal layer in 6-month-old AD mice as compared with littermate controls (Fig. 1a, Fig. S2a). The relative abundance of Aβ40 and Aβ42 in the GI tract (stomach, ileum and colon) was measured by ELISA analysis (Fig. 1b). The stomach and ileum of APP/PS1 mice were found to show significant intracellular Aβ deposition (Fig. S2b). Recent studies proposed that Aβ functions as an antibacterial peptide, which shows obvious inhibitory activity against a variety of pathogens [22]. Therefore, the intracellular Aβ deposition may be as a response to gut dysbiosis, and alteration in gut microbiota was considered to have occurred many years before the onset of AD [23]. Indeed, we also observed that the strong immunoreactivity of phosphorylated tau (p-Tau) existed in the myenteric plexuses of the APP/PS1 mice (Fig. S2c).

The Aβ42 immunoreactivity is co-localized in the mucosal layer CD68^{+} macrophages and myenteric HuC/D^{+} neurons (Fig. 1c, Fig. S3a). We found the number of CD68^{+} and Aβ42^{+}/CD68^{+} double-labeled macrophages increased significantly in the APP/PS1 mice (Fig. S3b). Macrophages, as the peripheral counterpart of microglia, have been shown to internalize and degrade various forms of Aβ [24]. Moreover, studies suggest that APP and its metabolites are involved in modulating CD68^{+} macrophage activation [19]. We observed an increase of Aβ immunoreactivity in myenteric HuC/D^{+} neurons in APP/PS1 mice (Fig. 1c, Fig. S3a, Fig. S3c). The proteins for Aβ generation were also overexpressed, such as the APP, beta-secretase (BACE1), and gamma-secretase (Presenilin1 and Nicastrin) (Fig. 1d, Fig. S3d). Furthermore, we found that more BACE1- and PSEN1-positive cells had intracellular Aβ deposition in the APP/PS1 mice by whole mount immunofluorescence
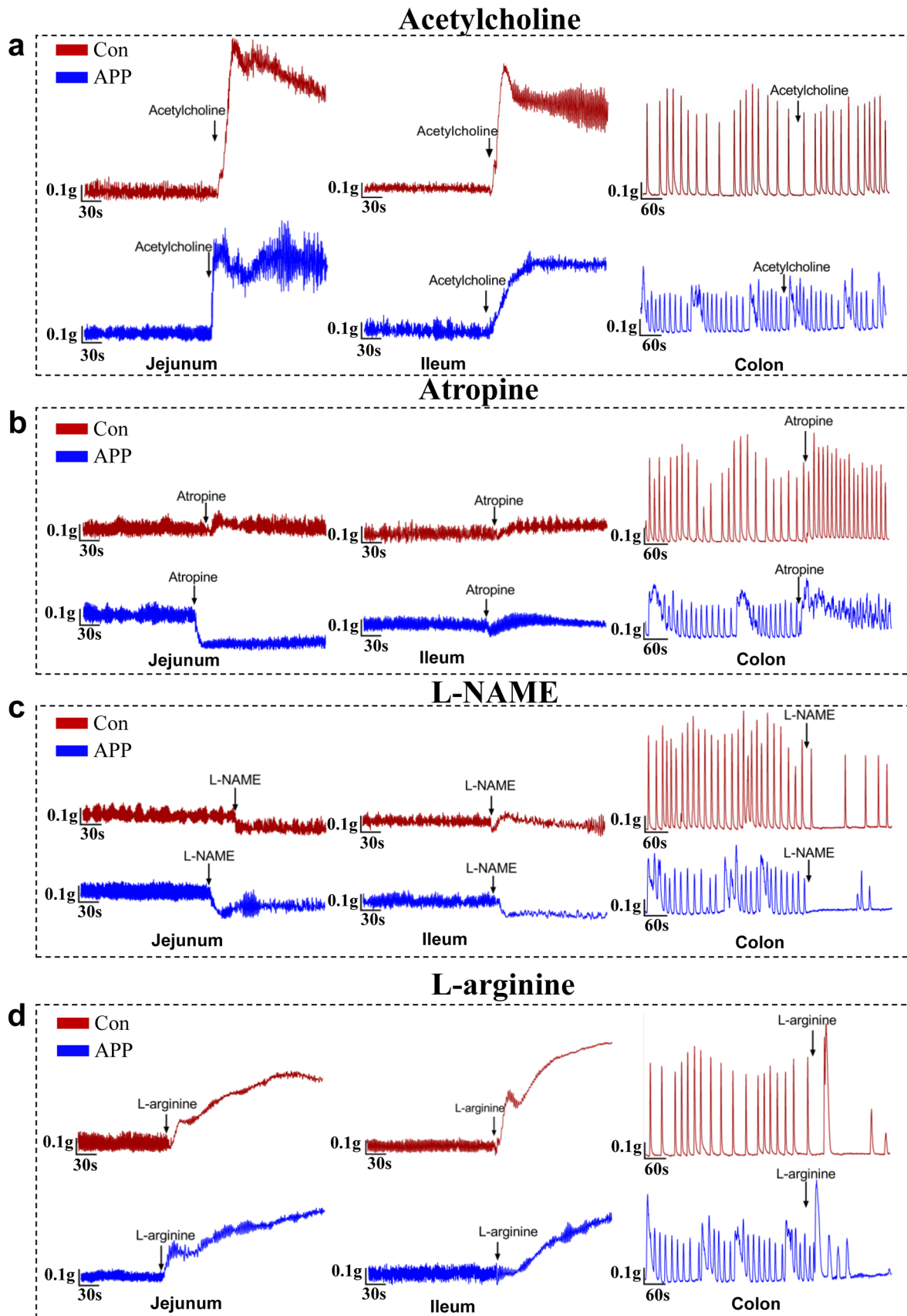
Acetylcholine

Atropine

L-NAME

L-arginine

◄**Fig. 2** The enteric cholinergic and nitric oxide signaling pathways were impaired in AD mice. **a**, **b** Representative tracing of acetylcholine-induced (**a**) and atropine-induced (**b**) muscle contraction in the intestinal segments from 3-month-old APP/PS1 and littermate controls. $N=4$/group. **c**, **d** Neuromuscular relaxation response induced by ʟ-NAME (**c**) and ʟ-arginine (**d**) in the isolated intestinal preparations from the 3-month-old APP/PS1 mice and littermate controls. $N=4$/group. Changes in muscle tension 5–10 min before and after exposure to each drug were measured. Drugs used in this study: 1 μmol/L of Acetylcholine; 50 μmol/L of Atropine; 10 mmol/L of ʟ-NAME of jejunum and ileum; 2 mmol/L of ʟ-NAME for colon; 15 mmol/L of ʟ-arginine

staining (Fig. S3e, Fig. S3f). Our results show an overexpression of Aβ in the ENS of AD mice. Intraneuronal Aβ deposition has been considered as a predictor for synaptic dysfunction and neuron loss in AD [25, 26]. Thus, Aβ deposition in the enteric neurons may result in intestinal dysfunction.

AD transgenic mice exhibit GI motility impairment

To investigate whether intestinal function was impaired with the intraneuronal Aβ deposition, we evaluated the gut transit time of AD mice. Our results suggest that 3-month-old APP/PS1 mice significantly decreased the average calculated geometric center of FITC-dextran fluorescence as compared with the littermate controls, showing an impairment in GI transit (Fig. 1e). Furthermore, our data show that GI transit impairment aggravates with aging (Fig. 1f). We observed that about 15% of the FITC-dextran remained in the stomach of APP/PS1 mice in contrast to 2.7% in littermate controls, indicating that gastric emptying capacity was impaired in 12-month-old APP/PS1 mice (Fig. 1f). In addition, AD mice show a tendency ($p=0.07$) to reduce the feces output at the age of 3 months, and this phenotype is more significant with age (Fig. 1g). Previous evidence suggests that AD patients are afflicted with a variety of GI symptoms [27], our results demonstrate that APP/PS1 mice have progressive intestinal dysfunction.

The cholinergic and nitric oxide signaling pathways were impaired in APP/PS1 mice

Neuronal control of GI motility mainly depends on the muscarinic cholinergic and nitric oxide (NO) signaling pathways [28]. To investigate whether intestinal dysfunction in APP/PS1 mice result from changes in enteric neurotransmissions, we evaluated the effect of acetylcholine (muscarinic agonist), atropine (muscarinic antagonist), ʟ-NAME (NO synthases inhibitor), ʟ-arginine (NO precursor), and potassium chloride (KCl) on intestinal contraction (Fig. 2a–d, Fig. S4). Our data showed that enteric cholinergic neurotransmission was damaged in 3-month-old APP/PS1 mice (Fig. 2a, b), as reflected in alteration of contractile tension and frequency

of intestinal smooth muscle evoked by acetylcholine and atropine (Fig. S5a–5b, Fig. S5e–5f). NO, as the major inhibitory neurotransmitter, plays an important role in regulating GI smooth muscle relaxation and motility [29]. We found that ʟ-NAME treatment significantly decreased intestinal muscle tension and contraction amplitude in APP/PS1 mice, while the response to ʟ-NAME in control specimens was less pronounced (Fig. 2c, Fig. S5c–5f). We observed that there were significant differences in response of intestinal segments to ʟ-arginine between the APP/PS1 mice and control groups (Fig. 2d, Fig. S5d–5f). Our data suggest that KCl, a stimulus reported to increase smooth muscle NO synthase activity in intestinal tissue [30], triggered different responses of smooth muscle between the APP/PS1 mice and littermate controls (Fig. S4, Fig. S5e–5g). Taking these data together, our results suggested that intestinal cholinergic and nitric oxide signaling pathway were impaired in the AD mice.

AD mice developed progressive enteric neuron loss and inflammation

To further investigate whether specific enteric neuron subtypes were damaged in AD mice, we evaluated the excitatory and inhibitory populations in myenteric plexus by immunohistochemistry. No significant difference in myenteric HuC/D$^+$ neurons was found in the colon between the APP/PS1 mice and littermate controls (Fig. 3a). We observed a higher proportion of VIP$^+$ neurons and a lower proportion nNOS$^+$ neurons in 3-month-old APP/PS1 mice (Fig. 3b, c). Western blot analysis suggested that the relative abundance of nNOS synthase, VIP peptide, and Calb1 protein was changed in AD mice as compared with the control group (Fig. 3d). Furthermore, we found that ENS damage was aggravated with aging. The neurons stained with anti-nNOS, anti-Chat, anti- Calb1, and anti-CR antibodies decreased significantly in the 12-month-old APP/PS1 mice (Fig. 3e, f), while VIP positive neurons remarkably increased as compared with the littermate controls (Fig. 3f, Fig. S6a). These morphological changes in the enteric neurons are also reflected at the protein level (Fig. S6b). The enteric nNOS$^+$ neurons play an important role in relaxing circular muscle to facilitate the movement of intestinal contents [31]. Deficits in nNOS$^+$ neurons have been observed in Hirschsprung's disease and Chagas' disease [32]. VIP, as a neurotransmitter, not only play an important role in regulating GI functions, but acts as an anti-inflammatory agent displaying neuroprotective effect [33].

We further investigated whether inflammation-related lesions also happened in colon, and found that increased inflammatory gene expression has appeared in the 3-month-old APP/PS1 mice (Fig. S6c). With the increase of age, AD mice showed a more significant up-regulation of inflammation-related proteins, such as the TLR4, p65 (NF-κB),
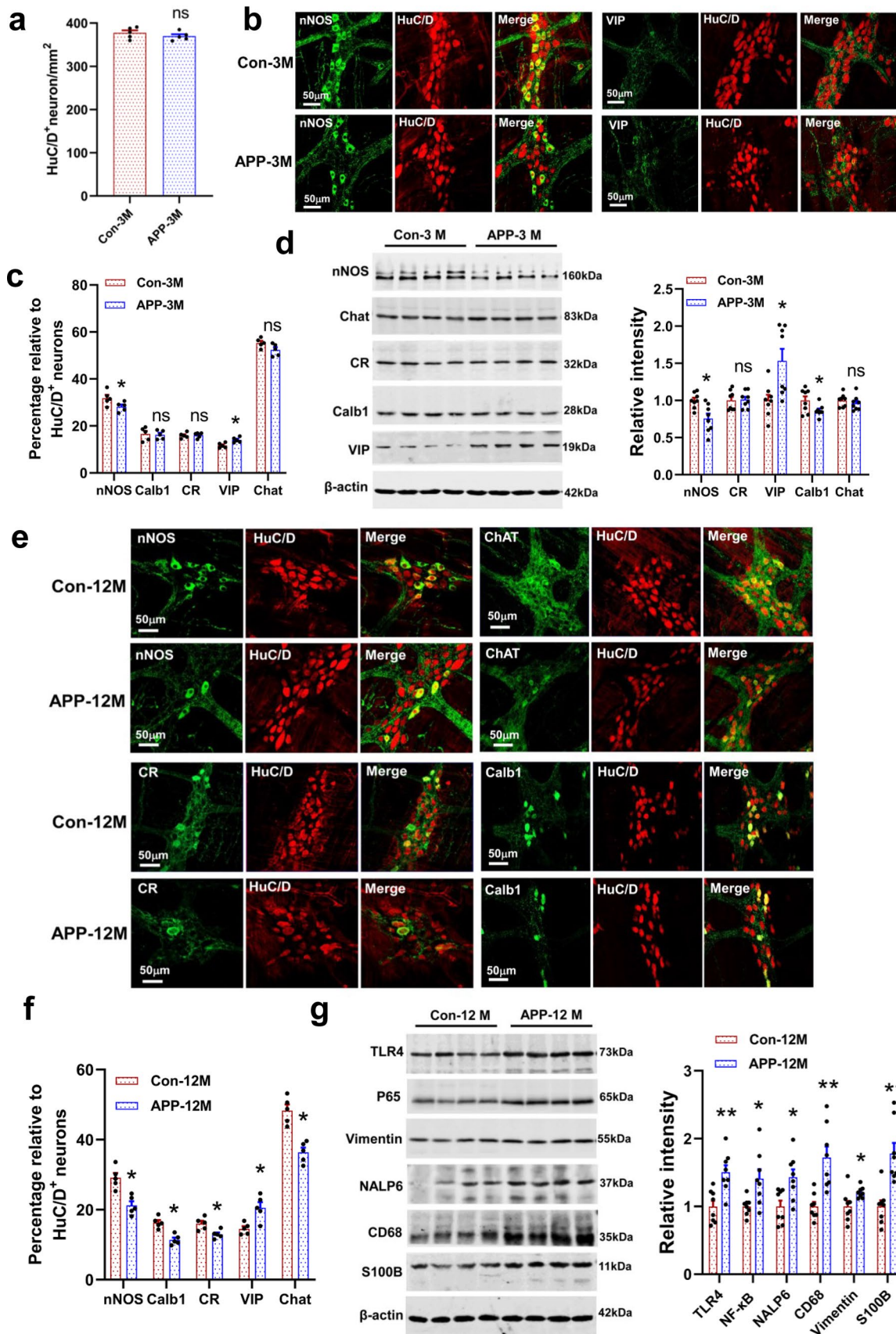
◄**Fig. 3** A gradual loss of colonic myenteric neurons and increase in inflammation-related proteins in the APP/PS1 mice. **a** Number of HuC/D$^+$ neurons were calculated in 3-month-old APP/PS1 mice and littermate controls based on the colonic whole mount staining. $N = 5$/group. Data are presented as mean ± SEM, unpaired t test, the "ns" represents no significance. **b** Representative micrographs of colonic whole mount staining for nNOS and VIP in 3-month-old APP/PS1 mice and littermate controls. $N = 5$/group. **c** Quantitative analysis of the major neuronal subtypes in the colonic myenteric plexus of 3-month-old APP/PS1 mice and littermate controls. $N = 5$/group. Data are presented as mean ± SEM, unpaired t test, *$P < 0.05$. The "ns" represents no significance. **d** Western blot assay for the expression profiles of nNOS, CR, VIP, Calb1 and Chat proteins in the colonic longitudinal muscle-myenteric plexus strips (LMMPs) from the 3-month-old APP/PS1 mice and littermate controls. $N = 8$/group. Data are presented as mean ± SEM, unpaired t test, *$P < 0.05$. **e** Representative micrographs of colonic whole mount staining for nNOS, Calb1, CR, and Chat in the 12-month-old APP/PS1 mice and littermate controls ($N = 5$/group). **f** Quantitative analysis of the major neuronal subtypes in the colonic myenteric plexus of 12-month-old APP/PS1 mice and littermate controls. $N = 5$/group. Data are presented as mean ± SEM, unpaired t test, *$P < 0.05$. **g** Western blot assay for the expression profiles of inflammation-associated proteins in the colonic LMMPs of the 12-month-old APP/PS1 mice and littermate controls. $N = 8$/group. Data are presented as mean ± SEM, unpaired t test, *$P < 0.05$

NLRP6, CD68, and S100B (Fig. 3g). TLR4, as the best characterized bacterial LPS receptor, has been found to modulate colonic motility and the survival of nNOS$^+$ neurons [34, 35]. We observed an increased immunoreactivity of TLR4 and phosphorylated p65 (p-p65) in HuC/D$^+$ myenteric neurons in APP/PS1 mice as compared with the littermate controls (Fig. S6d). Overactivation of p65 by TLR4 has been shown to be involved in caspase-11 mediated myenteric neuronal pyroptosis and colonic dysmotility [36]. Gut inflammation has been proposed to accelerate the Aβ plaque accumulation and neuronal damage in AD brains [9]. Our results provide further evidence for the pathological changes of AD include the ENS.

AD mice exhibited an impairment in neurogenesis and increased neuronal apoptosis and pyroptosis

To investigate whether ENS damages result from the impairment in enteric neurogenesis, we evaluated the expression of SOX2 and Nestin. The protein SOX2 is known as a marker of ENS progenitor cells [37], while Nestin is considered as the marker for neural stem cells [38]. Our data showed that the number of colonic Nestin$^+$/HuC/D$^+$ and SOX2$^+$/HuC/D$^+$ double-labeling neurons remarkably decreased in the APP/PS1 mice, compared with the littermate controls (Fig. 4a–c). Such changes in the expression levels of Nestin and SOX2 were further confirmed by western blotting analysis (Fig. 4d, Fig. S7a). Neuronal apoptosis and pyroptosis induced by activations of caspase proteins were regarded as an important cause of ENS impairment and GI disorders [36, 38,

39]. Analysis by Western blotting indicated that the expression of multiple apoptosis- and pyroptosis-related proteins increased significantly in the colon of APP/PS1 mice, compared with control group (Fig. 4d). Furthermore, this result was confirmed by immunofluorescence staining (Fig. 4e, f, Fig. S7b).

Accumulation of Aβ and bacterial LPS mediate the neuroinflammation and ENS changes

Aβ was considered as the trigger for synaptic loss, gliosis, and neuroinflammation in AD brains [40]. Is the ENS changes also related to the intraneuronal Aβ deposition? We first tested whether enteric neurons could take up Aβ peptide, and found that extracellular soluble FITC-labeled Aβ42 penetrated through the cell wall of enteric neurons and deposited in the neurons (Fig. 5a). Bacterial LPS, a gram-negative bacterial component, were higher in brains and serums of AD patients as compared to the control [41]. Our results also suggest that the level of LPS in feces and serum of APP/PS1 mice were significantly higher than those of control mice (Fig. 5b).

To investigate the effect of Aβ deposition and LPS, cultured enteric neurons (from 3-month-old wild-type mice) were treated with soluble Aβ42 (5 μM) or LPS (10 ng/mL) for 72 h, and then we evaluated their effects on colonic myenteric neuronal gene expression by qRT-PCR (Fig. 5c–e). We found that the mRNA levels of Aβ generation increased significantly in cultured myenteric neurons following the Aβ42 or LPS treatment (Fig. 5c). In addition, the apoptosis- and inflammation-related genes was also remarkably induced, such as the Caspase-3, Nlrp3, Tnf-α, Tlr2, Tlr4, and CD68 (Fig. 5d). More importantly, we found that Aβ42 or LPS exposure significantly changed the mRNA levels of several genes involved in neural activity and synaptic plasticity (Fig. 5e). We also tested the effect of LPS on cultured enteric neurons from 3-month-old APP/PS1 mice, and similar gene changes were observed (Fig. S8). It is noteworthy that up-regulation of nNOS expression has been reported to produce excessive NO, which promotes the neuronal death by increasing oxidative stress and intracellular calcium concentration, and inducing mitochondrial damage [42, 43]. While elevated VIP mRNA levels is usually considered as a protective action against Aβ-induced neurodegeneration [44]. Our results suggest that the accumulation of Aβ42 and LPS contributes to the neuropathological changes of enteric neurons in AD mice.

Intra-colon administration of Aβ impaired the GI motility and ENS function

We further investigate whether Aβ has a direct effect on GI motility, and found that both Aβ40 and Aβ42 treatment
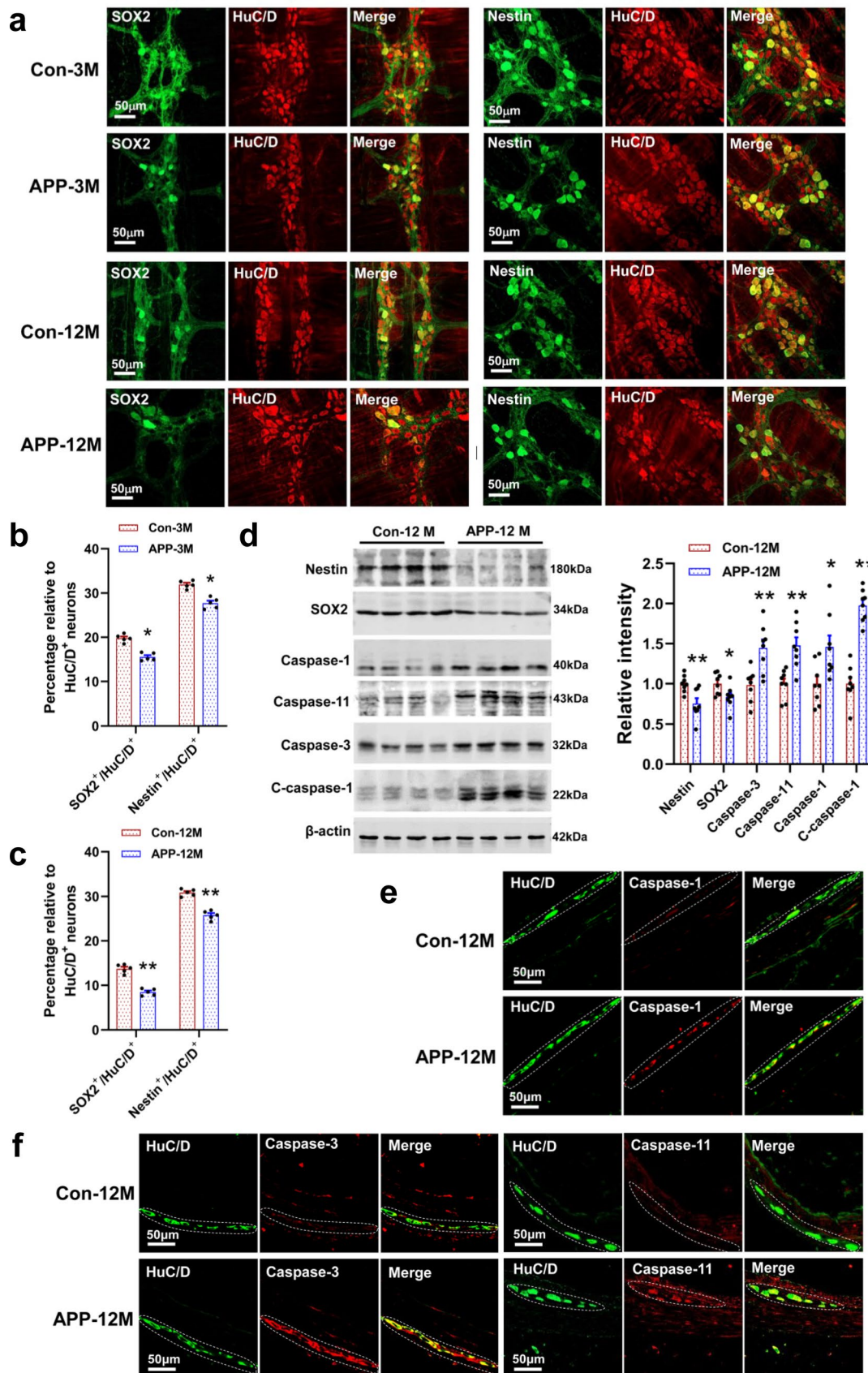
◄**Fig. 4** AD mice showed impaired neurogenesis and increased apoptosis and pyroptosis in enteric neurons. **a** Representative micrographs of colonic whole mount staining for SOX2 and Nestin from the 3- and 12-month-old APP/PS1 mice and littermate controls ($N = 5$/group). **b, c** Quantitative analysis shows that the number of SOX2$^+$/HuC/D$^+$ and Nestin$^+$/HuC/D$^+$ double-labeled neurons decreased in the colon of 3- and 12-month-old APP/PS1 mice and littermate controls. $N = 5$/group. Data are presented as mean ± SEM, unpaired t test, *$P < 0.05$, **$P < 0.01$. **d** Western blot analysis of the expression of proteins involved in neurogenesis, apoptosis, and pyroptosis from the LMMPs in the colon of APP/PS1 mice and littermate controls. $N = 8$/group. Data are presented as mean ± SEM, unpaired t test, *$P < 0.05$, **$P < 0.01$. **e, f** Representative micrographs show that the immunoreactivity of Caspase-1, Caspase-3, and Caspase-11 was significantly increased in the colonic myenteric plexus of 12-month-old APP/PS1 mice as compared with the littermate controls ($N = 5$/group). The results of quantitative analysis are shown in the Fig. S7

significantly decreased the spontaneous contractile tension of ileal and jejunal segments from the 3-month-old wild-type (WT) mice, and they also reduced the contraction frequency of colonic smooth muscle (Fig. 5f–h, Fig. S9). To our knowledge, this is the first report that Aβ has a direct effect on the contraction of intestinal smooth muscles, raising the possibility that Aβ plays an important role in modulating physiological function of GI tract.

To reveal the effects of Aβ on intestinal function in vivo, we injected the Aβ42 oligomer (2.5 μg/μL, 2 μL/location) into the serosa of colon at 3 sites of WT mice (3 months old) using a pulled glass pipette. After 9 months post-injection, our result showed that these 12-month-old Aβ-injected mice showed a longer bead latency time as compared with the vehicle-treated animals, indicating an impairment in colon motility (Fig. 6a). Furthermore, we found that the proportion of nNOS$^+$ neurons, Calb1$^+$ neuron, and CR$^+$ neuron significantly reduced in the Aβ-injected mice as compared with vehicle-treated control, while VIP$^+$ neurons remarkably increased (Fig. 6b, c). Consistent with this result, the expression of these proteins also changed accordingly (Fig. 6d). In addition, we found that intra-colon administration of Aβ42 impaired enteric neurogenesis and increased the apoptosis and inflammation, as reflected by changes the relative abundance of SOX2, Nestin, Caspase proteins, TLR4, and p65 (Fig. 6d, e). These results indicated that Aβ has a significant effect on modulating GI motility and ENS functions.

Intra-colon administration of Aβ caused cerebral β-amyloidosis

Previous studies suggested that intraperitoneal injection of Aβ-rich brain extracts enhanced cerebral β-amyloidosis in the brains of AD transgenic mice [45]. We investigated whether intra-colon administration of Aβ42 oligomers aggravates β-amyloidosis in APP/PS1 mice or triggers similar Aβ misfolding in brain of WT mice. The Aβ42 oligomers were injected into the colonic wall of the APP/PS1 or WT mice

(3 months old) using a pulled glass pipette, and pathological changes in the brain were detected at about 12 months of age. We performed immunofluorescence staining for Aβ, Iba-1, and GFAP, and found that Aβ-injected APP/PS1 mice not only remarkably enhanced the β-amyloid load in the hippocampus (Fig. 7a, Fig. S10), but also significantly increased astrocytosis and microgliosis as compared with the control group (Fig. 7b). We observed sporadic Aβ-like plaques and increased astrocytosis and microgliosis in the brain of WT mice injected with Aβ42 oligomers in the colon (Fig. 7). The intraneuronal Aβ40 and Aβ42 immunoreactivities, a predictor for synaptic dysfunction and neuron loss, significantly increased in the prefrontal cortex (PFC) and piriform cortex (Pir) in Aβ-injected WT mice as compared with the control group (Fig. S11). Consistent with previous studies, these areas were highly sensitive to Aβ accumulation, and were frequently reported to have the earliest amyloid-β aggregation and the Aβ immunoreactivity in several AD transgenic mice [46–48].

Discussion

AD is a neurodegenerative disorder featured by Aβ deposition and tau hyperphosphorylation [2]. The patients with mild cognitive impairment and AD often suffer from gastrointestinal symptoms, including GI inflammation, constipation and fecal incontinence [49]. Additionally, Crohn's disease and colitis have been associated with risk of developing anxiety, depression, and cognitive dysfunction [50]. These evidences put forward the possibility that GI tract may be also impaired in AD. However, the research on whether pathological features exist in the GI tract of AD patients is still very limited.

The critical manifestations of AD extend beyond the central nervous system

At present, the research on AD mainly focuses on the lesions of CNS. However, increasing evidence suggests that AD patients have a series of peripheral and systemic abnormalities [2, 51, 52]. In this study, we found a significant increased intracellular Aβ40 and Aβ42 immunoreactivity in the enteric neurons of AD mice, compared with the control group (Fig. 1, Fig. S2). Intraneuronal Aβ accumulation was considered as one of the earliest pathological events in AD, which was believed to appear before the extracellular amyloid plaques [25, 26]. Such kind of nonplaque-like Aβ immunoreactivity was also found in the intestinal tract of several AD mouse models [18, 53, 54]. No extracellular amyloid plaques in the intestine were observed may be due to the difference in APP isoforms, ratio of Aβ42 to Aβ40, and tissue microenvironment between the central and enteric neuron
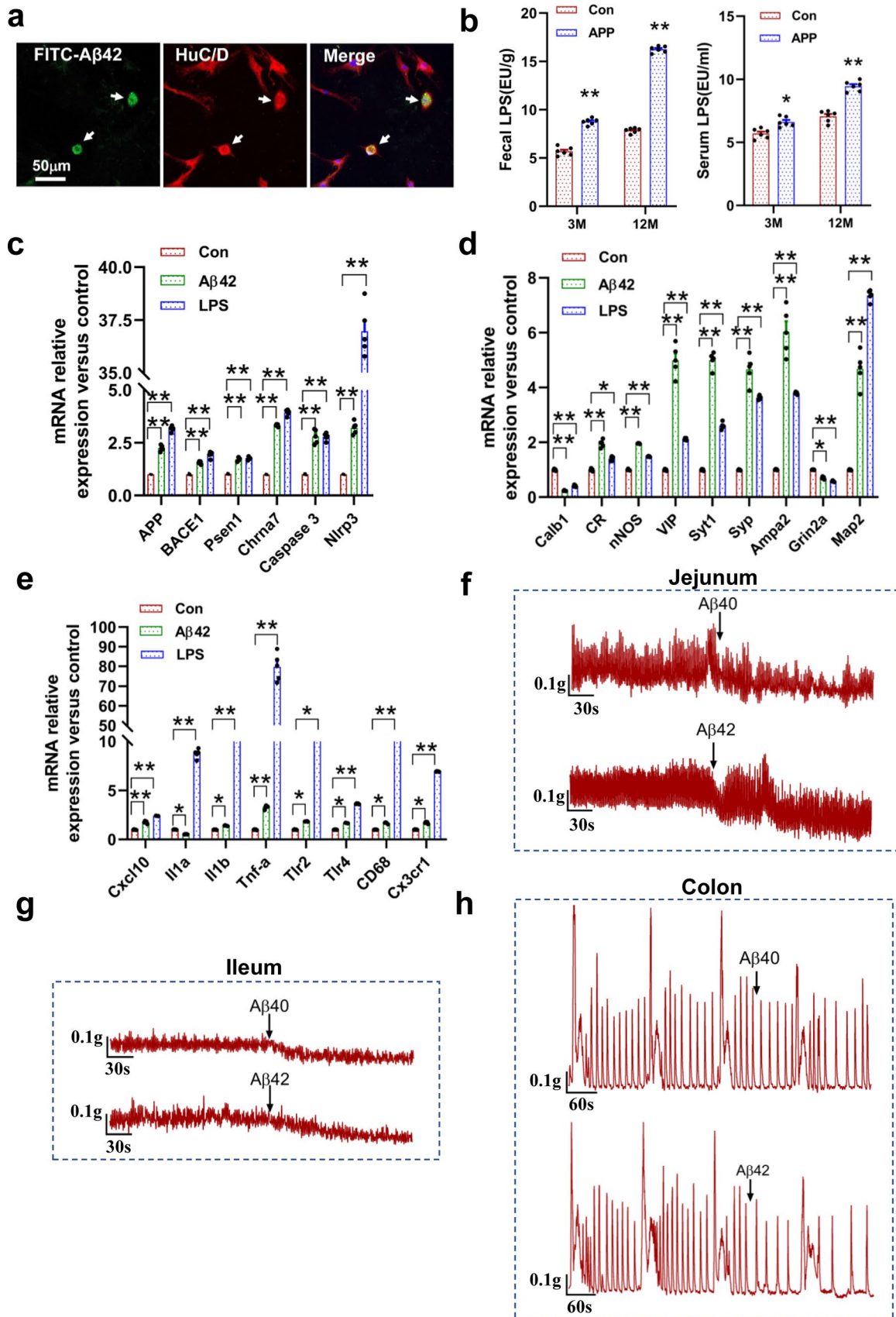
◄**Fig. 5** Aβ treatment has a significant effect on the gene expression of cultured myenteric neurons and spontaneous contraction of intestinal smooth muscle. **a** Representative micrographs show that cultured myenteric neurons took up FITC-labeled Aβ42. **b** Levels of bacterial LPS in the serum and feces from 3- and 12-month-old APP/PS1 mice and the littermate controls. $N = 6$/group. Data are presented as mean ± SEM. Statistical significance was determined using unpaired t test, *$P < 0.05$, **$P < 0.01$. **c–e** Analysis of the effects of soluble Aβ42 and LPS treatment on colonic myenteric neuronal gene expression by qRT-PCR. Cells from colonic myenteric plexus of 3-month-old WT mice were treated with 5 μM soluble Aβ42 or 10 ng/mL lipopolysaccharide (LPS) for 72 h. After that, treatment cells were collected for qRT-PCR. Data are presented as mean ± SEM. Statistical significance was determined using unpaired t test, *$P < 0.05$, **$P < 0.01$. **f–h** The effect of soluble Aβ40 and Aβ42 treatments on the spontaneous contraction of jejunal segments (**f**), ileal segments (**g**) and colonic segments (**h**) from 3-month-old WT mice, $N = 4$/group. Changes in muscle tension 5–10 min before and after exposure to each drug were measured. 20 μmol/L of Aβ42 and Aβ40 (Sigma-Aldrich)

systems. We also found a significant p-Tau immunoreactivity in the colonic myenteric plexus neurons of APP/PS1 mice as compared with the control group (Fig. S2c). Indeed, similar p-Tau immunoreactivity was also observed in another AD model mice, 3xTg triple transgenic mice (Fig. S12).

Another typical pathological feature in AD is microglia activation and enduring neuroinflammatory changes, which was found to contribute to synaptic stripping and neuronal loss [55]. The inflammatory changes were significant in the colon of APP/PS1 mice as verified by the elevated levels of serum and fecal LPS (Fig. 5b) and enhanced expression of CD68, TLR4, p65, Vimentin, and NLRP6 (Fig. 3g). The overexpression of p65 and TLR4 contributes to myenteric neuronal pyroptosis and colonic dysmotility [34, 36]. NLRP6 inflammasome was found to be involved in modulating innate immunity and colonic host–microbial interface [56, 57]. Synaptic degeneration and neuron loss is also a representative feature of AD. Here, we observed an impairment in GI transit and the cholinergic and NO signaling pathways in the APP/PS1 mice (Fig. 2). Recent studies have also reported GI transit damages in 5xFAD [58] and AppNL-G-F AD model mice [54]. Taken together, increasing evidence suggest that the typical pathological changes of AD also happen in the GI tract [59].

ENS as a target for AD neuropathology

Emerging evidence suggests that GI disorders are implicated in a series of neurodegenerative diseases, such as AD, PD, multiple sclerosis, and autism [6, 11]. Given many features shared between the ENS and the brain, the GI tract may also act a potential target of AD [60]. Over the last years, alterations in gut microbiota composition and gut inflammation have been proposed to be involved in amyloid and tau pathology in AD animal model [10, 61]. In this study, we

not only found intestinal dysfunction and increased inflammation in the colon of APP/PS1 mice, but also observed that the cholinergic neurons were lost with aging in myenteric plexus (Fig. 3e, f). Similar to our results, a recent study reported that enteric cholinergic neuromuscular pathway was damaged in SAMP8 AD model mice [62]. Selective loss of cholinergic neurons is a typical pathological feature in AD brains, and it was associated with Aβ accumulation [63]. The cholinergic neurons are the major excitatory subtype in the myenteric plexus, which are considered to be an important mediator of intestinal propulsion in rodents [64]. Additionally, our result showed that inhibitory signaling pathway was changed in the ENS of APP/PS1 mice, as reflected in decreasing the proportion of nNOS⁺ neurons and increasing VIP⁺ neurons (Fig. 3c, f). Nitrergic myenteric neurons are extremely susceptible to the pathological changes of the GI tract, and the loss or damage of these neurons has been reported in a series of diseases, including the AD [32, 65]. We also found that both Aβ40 and Aβ42 have a significant effect on the spontaneous rhythmicity of intestinal smooth muscles (Fig. 5f–h). These changes may be related to alteration of calcium signaling and (or) synaptic transmission in smooth muscle cells and enteric neurons [28]. Our results provide further evidence that ENS is also affected in AD.

Intestinal pathological changes may represent prodromal events for AD pathology

In this study, we found the robust intracellular Aβ42 deposition in the colon of young (3-month-old) APP/PS1 mice (Fig. 1c, Fig. S3c), while no obvious Aβ42 immunoreactivity was observed in the brains of the same animals (Fig. S13). Additionally, our results showed that young mice have exhibited GI motility impairment, intestinal inflammation, and ENS damage. Previous studies suggested that APP/PS1 mice show characteristic pathological changes, such as Aβ deposition and neuron loss, in the brains after 6 months of age [66, 67]. In other words, intestinal dysfunction and ENS damage may appeared before the typical pathological events in AD brains. Changes in gut microbiota has been observed in mild cognitive impairment patients before the onset of AD [23]. Moreover, gut dysbiosis was found to induce neuroinflammation, Aβ deposition and tau pathology in AD animal model [68]. The secretion of Aβ-peptides recently was considered as the result of bacterial infection and immune defense [22].

In addition, we found that intra-colon administration of Aβ42 oligomers induced ENS dysfunction (Fig. 6) and triggered Aβ deposition and gliosis in the brain of WT mice (Fig. 7). A recent study showed that gastrointestinal Aβ was translocate to the CNS via the vagus nerve [69]. Therefore, we evaluated whether the intra-colon injection of FITC-labeled Aβ42 oligomers could migrate to the CNS, and
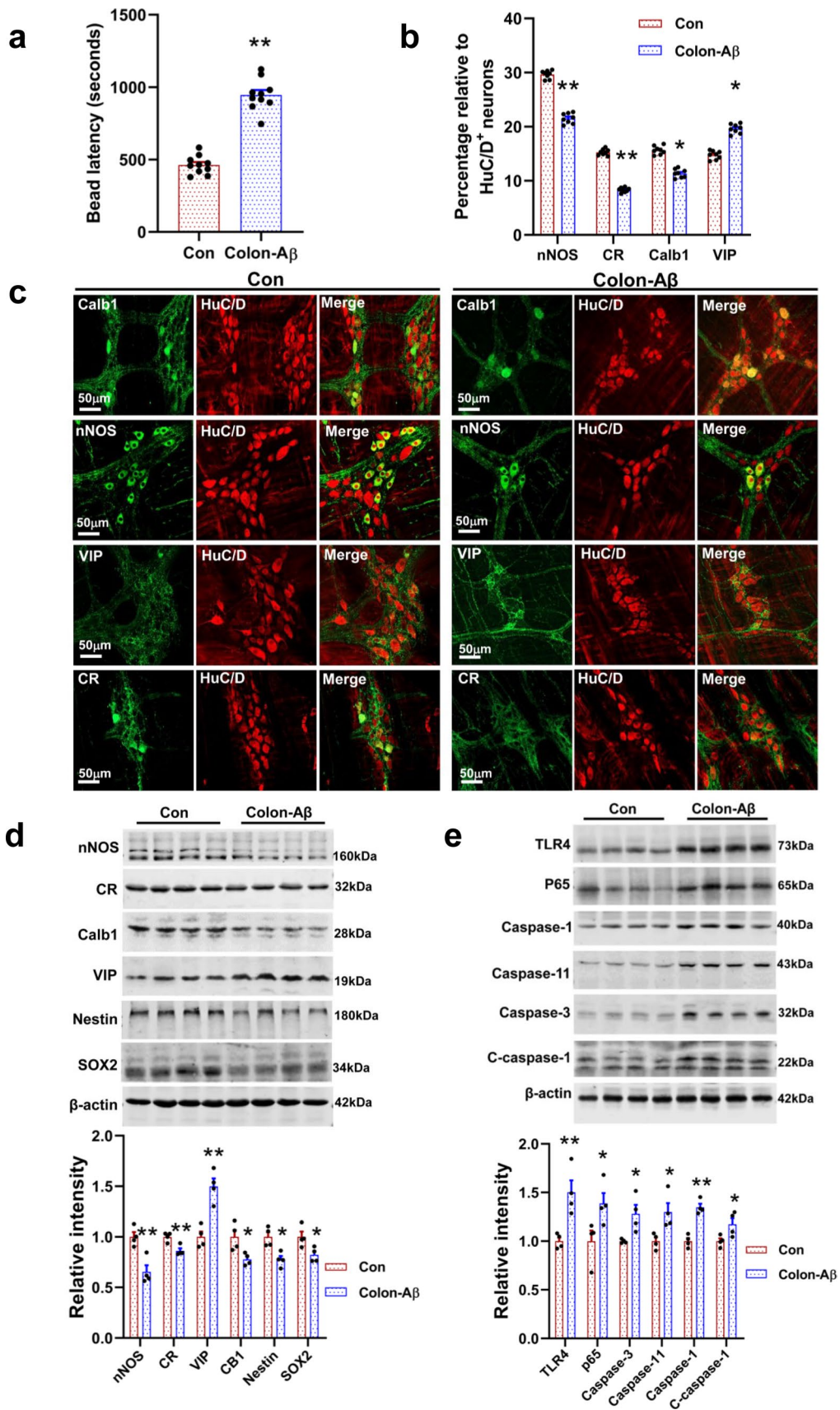
◂**Fig. 6** Intra-colon administration of Aβ42 oligomers leads to an increase of apoptosis and inflammation in enteric neurons. **a** Intra-colon administration of Aβ42 oligomers significantly increased the time required for colonic bead expulsion. 3-month-old WT mice were injected with Aβ42 oligomers in the proximal colon using a pulled glass pipette into the wall, $N=10$/group. At 9 months post-injection, these 12-month-old mice subject to colon motility test. Data are presented as mean ± SEM, unpaired t test, $**P < 0.01$. **b** Quantitative analysis of the relative proportion of CR$^+$, nNOS$^+$, VIP$^+$, and Calb1$^+$ neurons in colonic myenteric plexus from the Aβ42-treated mice and vehicle-treated control (12 months old). $N=8$/group. Data are presented as mean ± SEM, unpaired t test, $**P < 0.01$. **c** Representative micrographs of colonic whole mount staining for CR, nNOS, VIP, and Calb1 from the Aβ42-treated mice and vehicle-treated control (12 months old). $N=4$/group. **d** Western blot analysis of the proteins involved in neuroactivity and neurogenesis from the colonic longitudinal muscle-myenteric plexus strips of Aβ42-treated mice and vehicle-treated control (12 months old). $N=4$/group. Data are presented as mean ± SEM, unpaired t test, $*P < 0.05$, $**P < 0.01$. **e** Western blot analysis shows that the apoptosis- and inflammation-related proteins significantly increased in the colon of Aβ42-treated mice as compared with the control group. $N=4$/group. Data are presented as mean ± SEM, unpaired t test, $*P < 0.05$, $**P < 0.01$

found that no FITC fluorescent signal exists in the brain after 6 months post-injection (Fig. S14). We believe that the brain pathological changes induced by intra-colon administration of Aβ42 oligomers may be related to intestinal inflammation, gut dysbiosis and subsequent metabolic changes.

In summary, our results demonstrated that GI tract mirrors the typical pathological changes described in AD brains, emphasized the important role of Aβ in the ENS damage. We found that GI motility impairment, gut inflammation, and ENS damage probably represent prodromal events that precede analogous pathological events in AD brains. The GI tract acts as the major interface with the outside environment, our findings further raise the possibility that ENS acts as the potential portal for the pathogenesis of AD. Although more in-depth research is still needed, knowledge about the ENS changes in AD would pave the way for developing new strategies for early diagnosis and prevention.

Methods

Animals and treatment

C57BL/6J mice (wild-type), APP/PS1 double transgenic mice and 3xTg triple transgenic mice were originally obtained from Jackson Laboratory and were reared at a consistent ambient temperature (21 ± 1 °C) and humidity ($50 \pm 5\%$) with a 12-h light/dark cycle. Genotypes were confirmed by polymerase chain reaction analysis of genomic DNA isolated from tail biopsies. Experiments were mainly performed on 3- and 12-month-old male mice, except for the Fig. 1a, b (6 months old, male), Figs. S1, S2 (6 months old, male), and Fig. S14 (1 week old, 1 month old, and 6 months

old, male). The mice at these ages were selected mainly based on the time when Aβ deposition appears in APP/PS1 mice. For immunohistochemistry, brains, stomachs, ileums, and colons were isolated. For Aβ ELISA assay, tissues from cortex, stomach, jejunum, ileum, and proximal colon were homogenized in protein lysis buffer, and the supernatant was collected for analysis. For western blotting, proteins from proximal colon or longitudinal muscle-myenteric plexus (LMMP) strips from the proximal colon were prepared. All the procedures and treatments were conducted following the institutional guidelines and the Animal Care and Use Committee of the animal core facility at Huazhong University of Science and Technology, Wuhan, China.

Tissue preparation and immunohistochemistry

For LMMP preparations, 3- and 12-month-old APP/PS1 mice and their littermate controls were euthanized by cervical dislocation, the proximal colons were harvested and then fixed with 4% paraformaldehyde in PBS at room temperature for 1 h. LMMP was prepared by removing the mucosa, submucosa, and circular muscle layers under the dissecting microscope as previously described [70]. The paraffin-embedded stomach or intestinal (ileum, colon) tissues were cut into 4 μm thin sections and deparaffinized/rehydrated before performing immunostaining protocol. For brain sections, APP/PS1 mice and their littermate controls were deeply anesthetized and then perfused with 4% paraformaldehyde in PBS. Brains were removed and post-fixed in 4% PFA 24 h at 4 °C prior to immersing in the 30% sucrose solution. Fixed frozen sections were cut at 30 μm thickness using a cryostat (Leica).

For immunohistochemistry, antigen retrieval was performed by incubating the slides in citrate buffer at 95 °C for 20 min. LMMP preparations from the proximal colon or sections from the GI tract and brain were permeabilized with Triton X-100 (0.3%) in PBS for 30 min, and blocked with 3% bovine serum albumin (BSA) for 1 h. Then, these tissues were incubated for 48 h with the primary antibodies (Supplementary Table 1) at 4 °C followed by incubating in secondary antibodies for 2 h at room temperature. Cell nuclei were stained with DAPI, and the samples were visualized on Zeiss LSM800 confocal microscopes. To analyze the amyloid burden, the brain sections were stained with anti-Aβ40 antibody or anti-Aβ42 antibody and Thioflavin T. The number of Aβ plaques and the area fractions in the hippocampus were quantified with Image J software.

ELISA assay for Aβ levels determination

APP/PS1 mice and their littermate controls (6 months old) were killed by cervical dislocation, the cortexes, stomachs, jejunums, ileums, and proximal colons were removed and
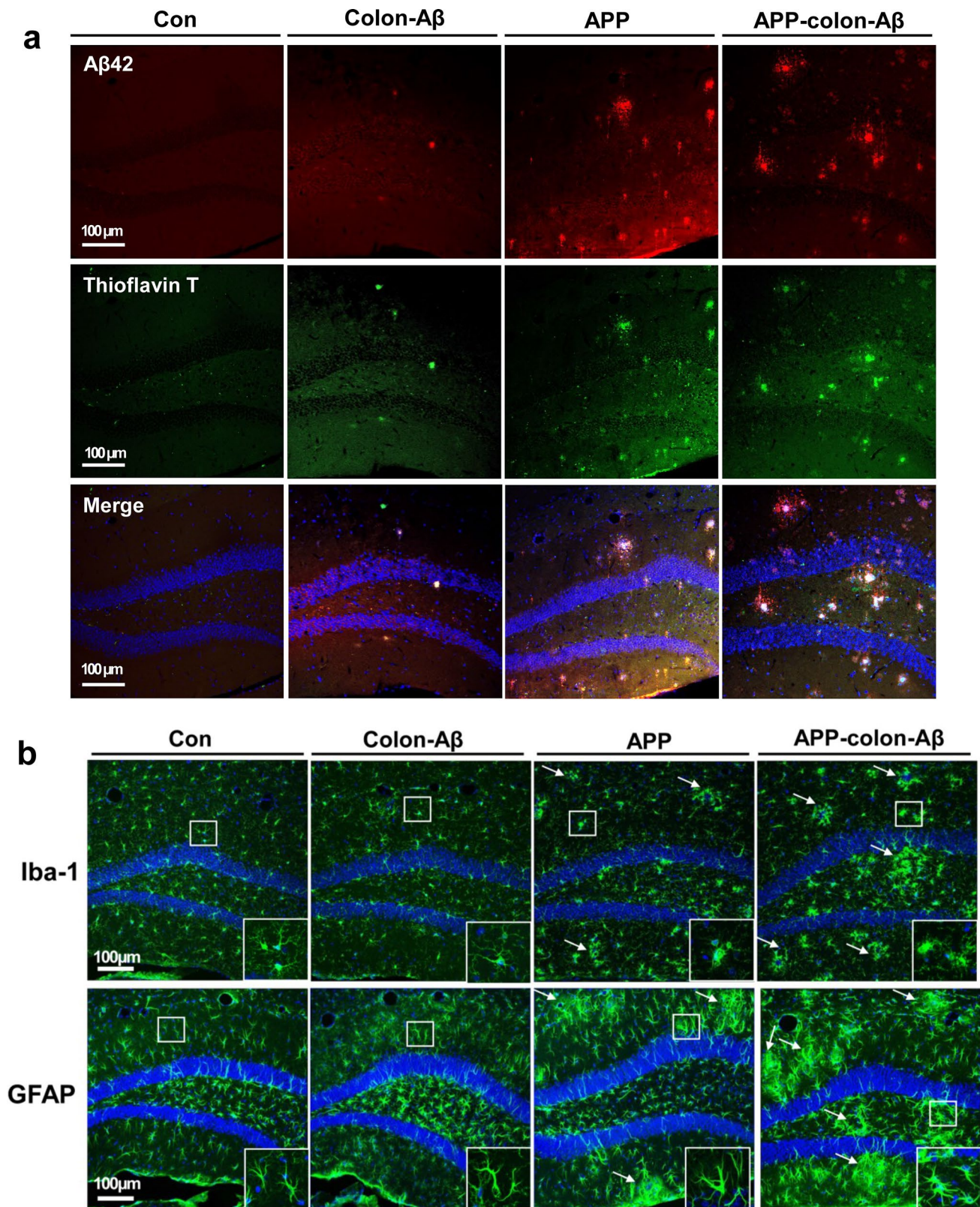
homogenized in RIPA buffer with protease inhibitors, and the supernatants were collected for quantifying the soluble Aβ40 and Aβ42. Aβ measurements were performed according to manufacturer's instructions using the commercially available Aβ40 (Elabscience, E-EL-H0542c) or Aβ42 ELISA kit (Elabscience, E-EL-H0543c). Aβ concentrations

◄**Fig. 7** Intra-colon administration of Aβ42 oligomers caused cerebral β-amyloidosis in the APP/PS1 and wild-type mice. **a** Representative micrographs show that typical Aβ plaques in the Aβ42-injected WT mice and Aβ42-injected APP/PS1 mice. 3-month-old mice were injected with Aβ42 oligomers in the proximal colon using a pulled glass pipette into the wall. Nine months later, these 12-month-old mice subject to a series of tests. The nucleuses were stained with DAPI; the amyloid-β plaque was stained with anti-Aβ42 antibody (Biolegend: 805501) and Thioflavin T. $N = 4$/group. **b** Representative micrographs show that the immunoreactivity of Iba-1 and GFAP in the hippocampus of Aβ42-injected mice and control group. The nucleuses were stained with DAPI; the astrocytes were stained with anti-GFAP antibody; the microglia were stained with anti-Iba-1 antibody. The arrow in the figure indicates the microglia aggregation and astrocytes aggregation. $N = 4$/group

in each animal were expressed as pg/mg protein. Protein content of tissues homogenates was calculated using the BCA Protein Assay Kit (Invitrogen). All samples were measured in triplicate, $N = 5$/group.

Western blotting

The proximal colons of mice (3- and 12 months old) were isolated from APP/PS1 mice and their littermate controls, $N = 4$–8/group. The proximal colons or the LMMP were homogenized in RIPA lysis buffer (10 mM Tris, pH 7.5, 150 mM NaCl, 1% deoxycholate, 1% NP40, 0.1% SDS, protease inhibitor cocktail). The supernatant was collected by centrifugation at 13,000 rpm for 10 min at 4 °C. After the protein concentrations were determined using BCA protein assay kit (Invitrogen), 25–40 μg of protein was resolved onto 10% (w/v) SDS-PAGE gel and transferred onto PVDF membrane (Millipore, USA) using a Mini Trans-Blot® Cell blot-apparatus (Bio-Rad). Membranes were blocked with 5% skimmed milk for 1 h and then incubated in the primary antibodies overnight at 4 °C. After the membranes were incubated with IRDye®800CW secondary antibodies (LI-COR Biosciences), the protein bands were scanned using the Odyssey® CLX Infrared Imaging System, and then quantified using the ImageJ software. The antibodies used are listed in Supplemental Table 1.

Gastrointestinal motility assay

The GI transit was assessed according to the methods described by Valentina Caputi et al. [71]. Briefly, APP/PS1 mice and their littermate controls (3- and 12 months old, $N = 6$/group) were gavaged orally with FITC-dextran (70 kDa; 25 mg/mL in 0.9% saline solution). After 30 min, the stomach and caecum were collected and examined separately, and the small intestine and the colon were cut into 10 and 2 equal segments, respectively. Then, the FITC-dextran intensity of each segment was measured at 492/521 nm. GI transit was determined by calculating the geometric center of FITC-dextran distribution using the following equation: GC = Σ (% of total fluorescent signal per segment × segment number)/100. The colonic motility was evaluated by the bead expulsion assay. A 3 mm glass bead was inserted into the distal colon (commonly from the anus 2 cm) of the 12-month-old Aβ42-injected APP/PS1 and the vehicle-treated mice ($N = 10$/group) using a glass rod pusher. The time required for colonic bead expulsion was then measured.

Measurement of intestinal contraction in vitro

3-month-old APP/PS1 mice and their littermate controls or WT mice were killed by cervical dislocation. The jejunum, ileum, and proximal colon were removed and placed in Krebs buffer solution bubbled continuously with 95% O_2 and 5% CO_2 at 37 °C. Luminal contents of the intestinal segments were flushed with Krebs buffer, and then 1.5 cm intestinal segments were mounted in 10 mL organ baths under 0.3 g tension equilibrated for 30 min in Krebs solution bubbled with 95% O_2 and 5% CO_2 (37 °C), while the Krebs solution was changed every 15 min. Changes in muscle tension 5–10 min before and after exposure to each drug were measured by isometric transducers connected to a PowerLab 8/35 system (ADInstruments, Australia). Before testing a new drug, intestinal segments were rinsed twice with fresh Krebs and were allowed to reach the steady baseline. The data was analyzed using the LabChart pro software (ADInstrument). Two–three replicates of each intestinal segment from the same animal were taken for testing, repeated in four animals for each drug in each group. Drugs used in this study: 1 μmol/L of Acetylcholine (Sigma-Aldrich); 50 μmol/L of Atropine (Topscience Co. Ltd); 10 mmol/L of L-NAME (Macklin Reagent Co. Ltd., China) for jejunum and ileum; 2 mmol/L of L-NAME for colon; 15 mmol/L of L-arginine and KCl (Macklin Reagent Co. Ltd., China); 20 μmol/L of Aβ42 and Aβ40 (Sigma-Aldrich). All drug were prepared before being used.

Measurement of bacterial LPS

The LPS levels of serum and feces from 3- and 12-month-old APP/PS1 mice and their littermate controls ($N = 6$/group) were measured using a commercial LPS ELISA kit (Mibio, Shanghai, China). Samples (serum and fecal supernatants) and LPS standard were plated onto a microplate pre-coated LPS capture antibody at room temperature. After incubation, the optical density (OD) was measured at 450 nm by automatic microplate reader, and the concentration of LPS in the samples was then determined by comparing the OD_{450} values of the samples to the standard curve.

Culture and treatment of enteric neurons.

Enteric neuron isolation and culture was performed according to Smith and colleagues with slight modification [72]. The proximal colon of WT mice or APP/PS1 mice (3 months old, male) were removed and kept in carbogen-gassed Krebs buffer. After the LMMP was prepared and digested, cells were seeded onto poly-D-lysine/laminin coated 12-well culture plates with 1 mL of culture media (Neurobasal A with B-27, 2 mM L-glutamine, 1% FCS, 10 ng/mL of GDNF, and 1% penicillin/streptomycin, 1% gentamicin/amphotericin). Cultures were maintained at 37 °C with 5% CO_2 throughout the experimental period. Cells were treated with 5 µM soluble Aβ42 or FITC-labeled Aβ42 (Sigma-Aldrich) or 10 ng/mL lipopolysaccharide (LPS, Sigma-Aldrich) for 72 h. The reason why we chose a concentration of 5 µM Aβ42 is mainly based on a large amount of literature [73–75]. A series of different concentrations of Aβ peptides have been used to treat various neuronal cell lines in vitro, such as 1 µM, 5 µM, 10 µM, and even 20 µM [40, 76]. After that, treatment cells were collected for real-time RT-PCR and immunohistochemistry.

Real-time RT-PCR

Cells treated with soluble Aβ42 and LPS were stored in RNAlater (Qiagen) at −80 °C until tissue processing. Total RNA was isolated according to the TRIzol extraction protocol (Invitrogen), and then reverse-transcribed into cDNA with PrimeScript™ RT reagent Kit with gDNA Eraser (Takara, China). Quantification RT-PCR was carried out using the SYBR Premix Ex Taq II Kit (Takara, China) in a Bio-Rad CFX-96 Detection System. The mRNA expressions were normalized to the housekeeping gene Actb, and calculated by $2^{-\Delta\Delta CT}$ methods. The sequences of primer used are described in Supplementary Table 2.

Intestinal intramuscular Aβ42 injection

Aβ42 oligomers were prepared according to the methods described by Fa et al. [77]. 3-month-old WT mice or APP/PS1 mice were anesthetized using isoflurane (2–4%), and then transferred to a sterile surgical pad with heating function. After sterilization of the abdomen, peritoneal cavity was exposed. The injections conducted using a pulled glass pipette into the wall (a depth of 1–2 mm) of the of proximal colon at 3 sites. A total of 5 µg of Aβ42 oligomers or FITC-Aβ42 (Sigma-Aldrich) at each site (2.5 µg/µL, 2 µL/location) was injected in the experimental group, and the equivalent volume of PBS was injected in control mice at the same locations. This operation was only performed once. Following this operation, the mice were sutured and returned to normal rearing conditions. Nine months after the intra-colon administration of Aβ, these mice (12 months old) subjected to a series of tests, such as colon motility test, pathological analysis of enteric neurons, and detection of Aβ deposition in cortex. The FITC-Aβ42 was used to track Aβ by immunofluorescence techniques.

Statistical analysis

All data were presented as means ± SEM, and the "N" refers to number of animals or the number of preparations involved for each figure. Statistical analyses were performed using the Graphpad Prism v8 for Windows (GraphPad Software Inc.). Differences between groups were analyzed by unpaired two-tailed t test or ANOVA with Bonferroni post hoc analysis, where appropriate. Significant differences were indicated in the figures by $*P < 0.05$, $**P < 0.01$, $***P < 0.001$.

Data availability All data generated or analyzed during this study are included in this published article (and its supplementary information files).

Declarations

Conflict of interest The authors declare no competing interests.

Ethics approval Animal experimental procedures were conducted following the institutional guidelines and the Animal Care and Use Committee of the animal core facility at Huazhong University of Science and Technology, Wuhan, China.

Consent to participate Not applicable.

Consent for publication All authors have read and approved the manuscript.

References

1. Cummings J, Lee G, Zhong K, Fonseca J, Taghva K (2021) Alzheimer's disease drug development pipeline: 2021. Alzheimers Dement (N Y) 7:e12179

2. Wang J, Gu BJ, Masters CL, Wang YJ (2017) A systemic view of Alzheimer disease—insights from amyloid-β metabolism beyond the brain. Nat Rev Neurol 13:612–623

3. Roher AE, Esh CL, Kokjohn TA, Castaño EM, Van Vickle GD, Kalback WM, Patton RL, Luehrs DC, Daugs ID, Kuo YM et al (2009) Amyloid beta peptides in human plasma and tissues and their significance for Alzheimer's disease. Alzheimers Dement 5:18–29

4. Sun HL, Chen SH, Yu ZY, Cheng Y, Tian DY, Fan DY, He CY, Wang J, Sun PY, Chen Y et al (2021) Blood cell-produced amyloid-β induces cerebral Alzheimer-type pathologies and behavioral deficits. Mol Psychiatry 26:5568–5577

5. Fung TC, Olson CA, Hsiao EY (2017) Interactions between the microbiota, immune and nervous systems in health and disease. Nat Neurosci 20:145–155

6. Niesler B, Kuerten S, Demir IE, Schäfer KH (2021) Disorders of the enteric nervous system—a holistic view. Nat Rev Gastroenterol Hepatol 18:393–410

7. Sohrabi M, Pecoraro HL, Combs CK (2021) Gut Inflammation induced by dextran sulfate sodium exacerbates amyloid-β plaque deposition in the AppNL-G-F mouse model of Alzheimer's disease. J Alzheimers Dis 79:1235–1255

8. Chen C, Ahn EH, Kang SS, Liu X, Alam A, Ye K (2020) Gut dysbiosis contributes to amyloid pathology, associated with C/EBPβ/AEP signaling activation in Alzheimer's disease mouse model. Sci Adv 6:eaba0466

9. Wu SC, Cao ZS, Chang KM, Juang JL (2017) Intestinal microbial dysbiosis aggravates the progression of Alzheimer's disease in Drosophila. Nat Commun 8:24

10. Kim MS, Kim Y, Choi H, Kim W, Park S, Lee D, Kim DK, Kim HJ, Choi H, Hyun DW et al (2020) Transfer of a healthy microbiota reduces amyloid and tau pathology in an Alzheimer's disease animal model. Gut 69:283–294

11. Chalazonitis A, Rao M (2018) Enteric nervous system manifestations of neurodegenerative disease. Brain Res 1693:207–213

12. Schneider S, Wright CM, Heuckeroth RO (2019) Unexpected roles for the second brain: enteric nervous system as master regulator of bowel function. Annu Rev Physiol 81:235–259

13. Wang L, Fleming SM, Chesselet M-F, Taché Y (2008) Abnormal colonic motility in mice overexpressing human wild-type α-synuclein. NeuroReport 19:873

14. Wang L, Magen I, Yuan PQ, Subramaniam SR, Richter F, Chesselet MF, Taché Y (2012) Mice overexpressing wild-type human alpha-synuclein display alterations in colonic myenteric ganglia and defecation. Neurogastroenterol Motil 24:e425–e436

15. Kim S, Kwon S-H, Kam T-I, Panicker N, Karuppagounder SS, Lee S, Lee JH, Kim WR, Kook M, Foss CA (2019) Transneuronal propagation of pathologic α-synuclein from the gut to the brain models Parkinson's disease. Neuron 103:627-641.e627

16. Wang X, Hu X, Yang Y, Takata T, Sakurai T (2016) Nicotinamide mononucleotide protects against β-amyloid oligomer-induced cognitive impairment and neuronal death. Brain Res 1643:1–9

17. Puig KL, Combs CK (2013) Expression and function of APP and its metabolites outside the central nervous system. Exp Gerontol 48:608–611

18. Puig KL, Lutz BM, Urquhart SA, Rebel AA, Zhou X, Manocha GD, Sens M, Tuteja AK, Foster NL, Combs CK (2015) Overexpression of mutant amyloid-β protein precursor and presenilin 1 modulates enteric nervous system. J Alzheimers Dis 44:1263–1278

19. Puig KL, Brose SA, Zhou X, Sens MA, Combs GF, Jensen MD, Golovko MY, Combs CK (2017) Amyloid precursor protein modulates macrophage phenotype and diet-dependent weight gain. Sci Rep 7:43725

20. Puig KL, Manocha GD, Combs CK (2015) Amyloid precursor protein mediated changes in intestinal epithelial phenotype in vitro. PLoS One 10:e0119534

21. Cabal A, Alonso-Cortina V, Gonzalez-Vazquez LO, Naves FJ, Del Valle ME, Vega JA (1995) beta-Amyloid precursor protein (beta APP) in human gut with special reference to the enteric nervous system. Brain Res Bull 38:417–423

22. Vojtechova I, Machacek T, Kristofikova Z, Stuchlik A, Petrasek T (2022) Infectious origin of Alzheimer's disease: amyloid beta as a component of brain antimicrobial immunity. PLoS Pathog 18:e1010929

23. Li B, He Y, Ma J, Huang P, Du J, Cao L, Wang Y, Xiao Q, Tang H, Chen S (2019) Mild cognitive impairment has similar alterations as Alzheimer's disease in gut microbiota. Alzheimers Dement 15:1357–1366

24. Zhao L, Lin S, Bales KR, Gelfanova V, Koger D, Delong C, Hale J, Liu F, Hunter JM, Paul SM (2009) Macrophage-mediated degradation of beta-amyloid via an apolipoprotein E isoform-dependent mechanism. J Neurosci 29:3603–3612

25. Welikovitch LA, Do Carmo S, Maglóczky Z, Malcolm JC, Lőke J, Klein WL, Freund T, Cuello AC (2020) Early intraneuronal amyloid triggers neuron-derived inflammatory signaling in APP transgenic rats and human brain. Proc Natl Acad Sci USA 117:6844–6854

26. Bayer TA, Wirths O (2010) Intracellular accumulation of amyloid-Beta—a predictor for synaptic dysfunction and neuron loss in Alzheimer's disease. Front Aging Neurosci 2:8

27. Khodabakhsh P, Bazrgar M, Dargahi L, Mohagheghi F, Asgari Taei A, Parvardeh S, Ahmadiani A (2021) Does Alzheimer's disease stem in the gastrointestinal system? Life Sci 287:120088

28. Sanders KM, Koh SD, Ro S, Ward SM (2012) Regulation of gastrointestinal motility—insights from smooth muscle biology. Nat Rev Gastroenterol Hepatol 9:633–645

29. Sanders KM, Ward SM (2019) Nitric oxide and its role as a non-adrenergic, non-cholinergic inhibitory neurotransmitter in the gastrointestinal tract. Br J Pharmacol 176:212–227

30. El-Yazbi AF, Cho WJ, Cena J, Schulz R, Daniel EE (2008) Smooth muscle NOS, colocalized with caveolin-1, modulates contraction in mouse small intestine. J Cell Mol Med 12:1404–1415

31. Beck K, Friebe A, Voussen B (2018) Nitrergic signaling via interstitial cells of Cajal and smooth muscle cells influences circular smooth muscle contractility in murine colon. Neurogastroenterol Motil 30:e13300

32. Bódi N, Szalai Z, Bagyánszki M (2019) Nitrergic enteric neurons in health and disease-focus on animal models. Int J Mol Sci 20:2003

33. Iwasaki M, Akiba Y, Kaunitz JD (2019) Recent advances in vasoactive intestinal peptide physiology and pathophysiology: focus on the gastrointestinal system. F1000Res. https://doi.org/10.12688/f1000research.18039.1

34. Anitha M, Vijay-Kumar M, Sitaraman SV, Gewirtz AT, Srinivasan S (2012) Gut microbial products regulate murine gastrointestinal motility via Toll-like receptor 4 signaling. Gastroenterology 143:1006-1016.e4

35. Caputi V, Marsilio I, Cerantola S, Roozfarakh M, Lante I, Galuppini F, Rugge M, Napoli E, Giulivi C, Orso G et al (2017) Toll-like receptor 4 modulates small intestine neuromuscular function through nitrergic and purinergic pathways. Front Pharmacol 8:350

36. Ye L, Li G, Goebel A, Raju AV, Kong F, Lv Y, Li K, Zhu Y, Raja S, He P et al (2020) Caspase-11-mediated enteric neuronal pyroptosis underlies Western diet-induced colonic dysmotility. J Clin Investig 130:3621–3636

37. Heanue TA, Pachnis V (2011) Prospective identification and isolation of enteric nervous system progenitors using Sox2. Stem Cells 29:128–140

38. Kulkarni S, Micci MA, Leser J, Shin C, Tang SC, Fu YY, Liu L, Li Q, Saha M, Li C et al (2017) Adult enteric nervous system in health is maintained by a dynamic balance between neuronal apoptosis and neurogenesis. Proc Natl Acad Sci USA 114:E3709–E3718

39. Kesavardhana S, Malireddi RKS, Kanneganti TD (2020) Caspases in cell death, inflammation, and pyroptosis. Annu Rev Immunol 38:567–595

40. Han XJ, Hu YY, Yang ZJ, Jiang LP, Shi SL, Li YR, Guo MY, Wu HL, Wan YY (2017) Amyloid β-42 induces neuronal apoptosis by targeting mitochondria. Mol Med Rep 16:4521–4528

41. Zhan X, Stamova B, Sharp FR (2018) Lipopolysaccharide associates with amyloid plaques, neurons and oligodendrocytes in Alzheimer's disease brain: a review. Front Aging Neurosci 10:42

42. Brown GC (2010) Nitric oxide and neuronal death. Nitric Oxide 23:153–165

43. Ghasemi M, Mayasi Y, Hannoun A, Eslami SM, Carandang R (2018) Nitric oxide and mitochondrial function in neurological diseases. Neuroscience 376:48–71

44. Delgado M, Varela N, Gonzalez-Rey E (2008) Vasoactive intestinal peptide protects against beta-amyloid-induced neurodegeneration by inhibiting microglia activation at multiple levels. Glia 56:1091–1103

45. Eisele YS, Obermüller U, Heilbronner G, Baumann F, Kaeser SA, Wolburg H, Walker LC, Staufenbiel M, Heikenwalder M, Jucker M (2010) Peripherally applied Abeta-containing inoculates induce cerebral beta-amyloidosis. Science 330:980–982

46. Zhang XM, Xiong K, Cai Y, Cai H, Luo XG, Feng JC, Clough RW, Patrylo PR, Struble RG, Yan XX (2010) Functional deprivation promotes amyloid plaque pathogenesis in Tg2576 mouse olfactory bulb and piriform cortex. Eur J Neurosci 31:710–721

47. Bero AW, Yan P, Roh JH, Cirrito JR, Stewart FR, Raichle ME, Lee JM, Holtzman DM (2011) Neuronal activity regulates the regional vulnerability to amyloid-β deposition. Nat Neurosci 14:750–756

48. Saiz-Sanchez D, Ubeda-Bañon I, De la Rosa-Prieto C, Martinez-Marcos A (2012) Differential expression of interneuron populations and correlation with amyloid-β deposition in the olfactory cortex of an AβPP/PS1 transgenic mouse model of Alzheimer's disease. J Alzheimers Dis 31:113–129

49. Rao M, Gershon MD (2016) The bowel and beyond: the enteric nervous system in neurological disorders. Nat Rev Gastroenterol Hepatol 13:517–528

50. Brooks AJ, Rowse G, Ryder A, Peach EJ, Corfe BM, Lobo AJ (2016) Systematic review: psychological morbidity in young people with inflammatory bowel disease - risk factors and impacts. Aliment Pharmacol Ther 44:3–15

51. Custodia A, Ouro A, Romaus-Sanjurjo D, Pías-Peleteiro JM, de Vries HE, Castillo J, Sobrino T (2021) Endothelial progenitor cells and vascular alterations in Alzheimer's disease. Front Aging Neurosci 13:811210

52. Zhuang ZQ, Shen LL, Li WW, Fu X, Zeng F, Gui L, Lü Y, Cai M, Zhu C, Tan YL et al (2018) Gut microbiota is altered in patients with Alzheimer's disease. J Alzheimers Dis 63:1337–1346

53. Feng J, Dong L, Zhang J, Han X, Tang S, Song L, Cong L, Wang X, Wang Y, Du Y (2018) Unique expression pattern of KIBRA in the enteric nervous system of APP/PS1 mice. Neurosci Lett 675:41–47

54. Manocha GD, Floden AM, Miller NM, Smith AJ, Nagamoto-Combs K, Saito T, Saido TC, Combs CK (2019) Temporal progression of Alzheimer's disease in brains and intestines of transgenic mice. Neurobiol Aging 81:166–176

55. Li JW, Zong Y, Cao XP, Tan L, Tan L (2018) Microglial priming in Alzheimer's disease. Ann Transl Med 6:176

56. Wlodarska M, Thaiss CA, Nowarski R, Henao-Mejia J, Zhang JP, Brown EM, Frankel G, Levy M, Katz MN, Philbrick WM et al (2014) NLRP6 inflammasome orchestrates the colonic host-microbial interface by regulating goblet cell mucus secretion. Cell 156:1045–1059

57. Anand PK, Malireddi RK, Lukens JR, Vogel P, Bertin J, Lamkanfi M, Kanneganti TD (2012) NLRP6 negatively regulates innate immunity and host defence against bacterial pathogens. Nature 488:389–393

58. Stoye NM, Dos Santos Guilherme M, Endres K (2020) Alzheimer's disease in the gut-Major changes in the gut of 5xFAD model mice with ApoA1 as potential key player. FASEB J 34:11883–11899

59. Sohrabi M, Sahu B, Kaur H, Hasler WA, Prakash A, Combs CK (2022) Gastrointestinal changes and Alzheimer's disease. Curr Alzheimer Res 19:335–350

60. Furness JB, Stebbing MJ (2018) The first brain: species comparisons and evolutionary implications for the enteric and central nervous systems. Neurogastroenterol Motil. https://doi.org/10.1111/nmo.13234

61. Chen C, Zhou Y, Wang H, Alam A, Kang SS, Ahn EH, Liu X, Jia J, Ye K (2021) Gut inflammation triggers C/EBPβ/δ-secretase-dependent gut-to-brain propagation of Aβ and Tau fibrils in Alzheimer's disease. EMBO J 40:e106320

62. Pellegrini C, Daniele S, Antonioli L, Benvenuti L, D'Antongiovanni V, Piccarducci R, Pietrobono D, Citi V, Piragine E, Flori L et al (2020) Prodromal intestinal events in Alzheimer's disease (AD): colonic dysmotility and inflammation are associated with enteric AD-related protein deposition. Int J Mol Sci 21:3523

63. Hampel H, Mesulam MM, Cuello AC, Farlow MR, Giacobini E, Grossberg GT, Khachaturian AS, Vergallo A, Cavedo E, Snyder PJ et al (2018) The cholinergic system in the pathophysiology and treatment of Alzheimer's disease. Brain 141:1917–1933

64. Delvalle NM, Fried DE, Rivera-Lopez G, Gaudette L, Gulbransen BD (2018) Cholinergic activation of enteric glia is a physiological mechanism that contributes to the regulation of gastrointestinal motility. Am J Physiol Gastrointest Liver Physiol 315:G473–G483

65. Han X, Tang S, Dong L, Song L, Dong Y, Wang Y, Du Y (2017) Loss of nitrergic and cholinergic neurons in the enteric nervous system of APP/PS1 transgenic mouse model. Neurosci Lett 642:59–65

66. Reiserer RS, Harrison FE, Syverud DC, McDonald MP (2007) Impaired spatial learning in the APPSwe + PSEN1DeltaE9 bigenic mouse model of Alzheimer's disease. Genes Brain Behav 6:54–65

67. Sadowski M, Pankiewicz J, Scholtzova H, Ji Y, Quartermain D, Jensen CH, Duff K, Nixon RA, Gruen RJ, Wisniewski T (2004) Amyloid-beta deposition is associated with decreased hippocampal glucose metabolism and spatial memory impairment in APP/PS1 mice. J Neuropathol Exp Neurol 63:418–428

68. Zhang Y, Geng R, Tu Q (2021) Gut microbial involvement in Alzheimer's disease pathogenesis. Aging (Albany NY) 13:13359–13371

69. Sun Y, Sommerville NR, Liu JYH, Ngan MP, Poon D, Ponomarev ED, Lu Z, Kung JSC, Rudd JA (2020) Intra-gastrointestinal amyloid-β1-42 oligomers perturb enteric function and induce Alzheimer's disease pathology. J Physiol 598:4209–4223

70. Brun P, Giron MC, Qesari M, Porzionato A, Caputi V, Zoppellaro C, Banzato S, Grillo AR, Spagnol L, De Caro R et al (2013) Toll-like receptor 2 regulates intestinal inflammation by controlling integrity of the enteric nervous system. Gastroenterology 145:1323–1333

71. Caputi V, Marsilio I, Filpa V, Cerantola S, Orso G, Bistoletti M, Paccagnella N, De Martin S, Montopoli M, Dall'Acqua S et al (2017) Antibiotic-induced dysbiosis of the microbiota impairs gut neuromuscular function in juvenile mice. Br J Pharmacol 174:3623–3639

72. Smith TH, Ngwainmbi J, Grider JR, Dewey WL, Akbarali HI (2013) An in-vitro preparation of isolated enteric neurons and glia from the myenteric plexus of the adult mouse. J Vis Exp 78:50688

73. Hou TT, Yang HY, Wang W, Wu QQ, Tian YR, Jia JP (2018) Sulforaphane inhibits the generation of amyloid-β oligomer and promotes spatial learning and memory in Alzheimer's disease (PS1V97L) transgenic mice. J Alzheimers Dis 62:1803–1813

74. Dorey E, Bamji-Mirza M, Najem D, Li Y, Liu H, Callaghan D, Walker D, Lue LF, Stanimirovic D, Zhang W (2017) Apolipoprotein E isoforms differentially regulate Alzheimer's disease and amyloid-β-induced inflammatory response in vivo and in vitro. J Alzheimers Dis 57:1265–1279

75. Li M, Liu E, Zhou Q, Li S, Wang X, Liu Y, Wang L, Sun D, Ye J, Gao Y et al (2018) TRPC1 null exacerbates memory deficit and apoptosis induced by amyloid-β. J Alzheimers Dis 63:761–772

76. Chen S, Jia J (2020) Tenuifolin attenuates amyloid-β42-induced neuroinflammation in microglia through the NF-κB signaling pathway. J Alzheimers Dis 76:195–205

77. Fa M, Orozco IJ, Francis YI, Saeed F, Gong Y, Arancio O (2010) Preparation of oligomeric beta-amyloid 1–42 and induction of synaptic plasticity impairment on hippocampal slices. J Vis Exp 41:1884